Journal of Statistical Physics, Vol. 46, Nos. 3/4, 1987

Shock Compression of Simple Molecules

M. S. Abdelazim[1]

Received July 29, 1986; revision received October 15, 1986

A simple approach is developed to calculate shock compression of simple molecules. This approach is based upon an accurate analytic representation of the Lennard-Jones fluids in conjunction with the Enskog theory, which is used to calculate the molecular diameter as a function of temperature along the Hugoniot. The model permits rapid, yet reliable calculations. It is applied to N_2, O_2, H_2, D_2, CH_4, CO, and CO_2. The results are tested by the comparison with experimental data and with other calculations. The computed Hugoniots agree reasonably with experimental results for many (but not all) simple molecules and are comparable to those of more complicated models.

KEY WORDS: Shock compression; simple molecules, dense fluids; Lennard-Jones; Enskog theory.

1. INTRODUCTION

The molecular species CO_2, CO, O_2, N_2, H_2, and CH_4 constitute most of the detonation products of the majority of explosives used in practice and in experimental investigations.[1] If the different dynamic and thermodynamic aspects of the pure components of explosives are defined at high pressures and densities (conditions attained by shock compression), the properties of the aggregate could be predicted. The determination of shock parameters that are used to determine the initiation process and the detonation hazards requires knowing the shock Hugoniot of the unreacted explosive. Also, shock compression analysis of H_2 and D_2 is of great importance in modeling planetary interiors and fusion problems.

Shock compression of the above-mentioned simple molecules is also of particular theoretical interest. Modern theories of statistical mechanics can be applied to them to perform reasonably rigorous calculations.

A large body of experimental data on shock compression of simple

[1] Department of Physics, University of Assiut, Assiut, Egypt.

0022-4715/87/0200-0635$05.00/0

molecules is now available.[2–5] However, for a fundamental understanding of the physical behavior of these molecules under the extreme conditions of high temperatures and densities, reliable theoretical calculations that assume realistic intermolecular potentials are required. Many attempts[6–12] have been made to construct such rigorous calculations. The approach is usually based upon the assumption of the additivity of intermolecular energy of isolated pairs and fluid perturbation theory.

The fact that the liquid structure is primarily determined by the short-range repulsive force and the relatively long-range attractive part suggested that the fluid can be treated as a system of molecules governed by a repulsive potential and an attractive part that can be treated as a small perturbation. Among the best perturbation theories are those of Barker and Henderson (BH) and Weeks, Chandler, and Anderson (WCA).[13] These theories, however, use the hard-sphere potential as a reference system, which introduces repulsion that tends to be severe at high density and temperature, i.e., at small separation. In order to overcome this difficulty, Ross[7] used a variational perturbation technique that employs the softer inverse 12th power repulsion as the reference potential to calculate shock compression of argon. His calculations were compared with experimental data and used to assess the accuracy of the repulsive potential of argon. He reproduced the shock data of liquid argon using the exponential-six (exp-6) potential with the parameters $\alpha = 13.0$, $\varepsilon/k = 122$ K, and $r^* = 3.85$ Å.

Using the corresponding state theory in conjunction with the parameters r^* and ε/k for argon, Ross and Ree[9] gave a simple recipe to evaluate the parameters r^* and ε/k for N_2, O_2, CO, CO_2, and CH_4. They also discussed the possibility that the repulsive pair potential of these fluids scale in accordance with the "law of corresponding state." They found that this law to be approximately valid to a compression of about 2.5 times liquid density.

It is often the case in such theoretical modeling of shock compression of simple molecules that investigators attempt to determine individually the relevant pair potential for each molecular species with the parameters that produce the experimental Hugoniot data. In the present calculations an analytic representation of the thermodynamic data for Lennard-Jones (LJ) fluids developed by Hansen[14] and Ree[15] is used to calculate shock compressions of simple molecules.

Although this relatively simple expression fits "experimental" thermodynamic data quite well over a wide range of density and temperature and permits a rapid evaluation of thermodynamic quantities, the Lennard-Jones potential tends to be very stiff at small separations. Consequently, shock compression calculations based upon this expression diverge severely at high densities, predicting much higher pressures.

In order to overcome this difficulty and take advantage of the convenience of using an analytic form for the equation of state, we introduced the Enskog theory to calculate the "collisional" separation σ as a function of temperature along the Hugoniot. This idea was inspired by the fact that, at high temperatures, molecules approach and scatter at much smaller distances. Therefore, it makes sense to think about the separation distance as being a function of temperature instead of treating it as a constant parameter along the Hugoniot. In fact, the Enskog theory provides such a functional dependence quite nicely in terms of a simple analytic expression. Therefore, the object of the present work is to present a simple, yet reliable approach for rapid computational calculations of shock compression for simple molecules. Also, the study sheds further light on the nature of the intermolecular forces at conditions attained by shock waves.

It is worth saying that this approach is quite applicable to other spherical potentials, e.g., exp-6. In fact, calculations that employ the same idea in conjunction with the fluid variational perturbation theory and the exp-6 potential are in progress.

In the next section we present the theoretical formulation of the model. Section 3 is devoted to presentation and discussion of the results. Section 4 provides a brief summary.

2. THEORETICAL FORMULATION

The passage of a shock wave through matter produces a large increase in its density, temperature, and pressure. In a typical shock experiment these thermodynamic quantities are not directly measurable. The Hugoniot data are generated by performing a series of experiments that measure shock velocity U_s and particle or material velocity U_p.

The thermodynamic and hydrodynamic states in the cold and hot sides of the shock front are related through the conservation relations. For a coordinate system moving with the shock, these relations are

$$\rho_0 U_0 = \rho_1 U_1 \qquad \text{(mass)} \tag{1}$$

$$P_0 + \rho_0 U_0^2 = P_1 + \rho_1 U_1^2 \qquad \text{(momentum)} \tag{2}$$

$$E_0 + P_0/\rho_0 + \tfrac{1}{2}U_0^2 = E_1 + P_1/\rho_1 + \tfrac{1}{2}U_1^2 \qquad \text{(energy)} \tag{3}$$

where $U_0 = U_s$ and $U_1 = U_s - U_p$. Here, E, P, and ρ are, respectively, the total specific internal energy (energy per unit mass), pressure, and density. Subscript 0 refers to the initial (cold) state and subscript 1 refers to the final (hot) state.

Eliminating the velocities from the above relations leads to the Hugoniot relation

$$E_1 - E_0 = \tfrac{1}{2}(P_0 + P)(V_0 - V_1) \tag{4}$$

where V is the specific volume ($V = 1/\rho$). The Hugoniot relation gives the locus of all possible final states of compression for a given initial state.

The application of the hydrodynamic theory to the determination of the shock Hugoniot requires a complete thermodynamic description of the molecular system. A useful representation of fluid properties can be based upon the Lennard-Jones (6–12) potential

$$\phi(r) = 4\varepsilon[(\sigma/r)^{12} - (\sigma/r)^6] \tag{5}$$

where ε is the depth of the potential and σ is the "collisional" separation distance at which the potential vanishes.

Based upon this potential, Hansen[14] and Ree[15] developed the following expression for pressure:

$$\beta P/\rho = \beta P_{\text{rep}}/\rho - (1/T^*)^{1/2} \sum_{i=1}^{5} iC_i X^i + (1/T^*) \sum_{i=1}^{5} D_i X^i \tag{6}$$

where

$$\beta P_{\text{rep}}/\rho = 1 + B_1 X + B_2 X^2 + B_3 X^3 + B_4 X^4 + B_{10} X^{10}$$

where $\beta = 1/kT$ and $X = \rho^*/T^{*1/4}$, where $\rho^* = N\sigma^3/V$ and $T^* = kT/\varepsilon$. The first two terms of the above expression are those of Hansen, who treated the repulsive part of the LJ potential $4\varepsilon(\sigma/r)^{12}$ as the reference potential and the attractive part as a perturbation. The first term in Eq. (6) corresponds to the repulsive reference potential and the second term represents the leading high-temperature correction of the attraction. Hansen's values for the least-square fit are $B_1 = 3.629$, $B_2 = 7.2641$, $B_3 = 10.4924$, $B_4 = 11.459$, $B_{10} = 2.17619$, $C_1 = 5.3692$, $C_2 = 6.5797$, $C_3 = 6.1745$, $C_4 = -4.2685$, and $C_5 = 1.6841$. His expression [the first two terms of Eq. (6)] is in excellent agreement with the exact Monte Carlo computations down to about twice the critical temperature ($T_c^* = 2.75$). By including the low-temperature Monte Carlo and molecular dynamics data, Ree[15] extended the range of the LJ equation of state to about the triple point ($T_t^* = 0.68$). The third term in Eq. (6) is Ree's contribution. Ree's values for the fitting parameters are $D_1 = -3.4921$, $D_2 = 18.6980$, $D_3 = -35.5049$, $D_4 = 31.8151$, and $D_5 = -11.1953$. The Hansen–Ree equation of state was very useful in calculating the wave structure of dense-fluid detonation[16] and detonation performance.[17]

In spite of the convenience of the analytic property and usefulness of the Hansen–Ree equation of state, its main failing is that it bears the same property of stiffness and inflexibility as the Lennard-Jones potential at small separations. In order to overcome this difficulty, the Enskog theory[18] is used to calculate the "collision" separation σ as a function of temperature along the Hugoniot.

In dense fluids made up of molecules of finite size, the frequency of collision is increased by a factor Y from that of a dilute gas made up of molecules whose molecular diameter σ is small compared to the mean free path. Enskog suggested that the equation of state of a dense fluid be written in the form

$$PV/RT = 1 + (b_0/V)\, Y \tag{7}$$

where $b_0 = \frac{2}{3}\pi N\sigma^3$.

Although the above formula was obtained for a gas composed of rigid spherical molecules, Enskog showed that it can be applied to real molecules if the pressure in Eq. (7) is replaced by the thermal pressure, which is given by

$$P_{\text{th}} = T(\partial P/\partial T)_V = (\partial E/\partial V)_T + P \tag{8}$$

i.e., Enskog supposed that the real, dense gas is equivalent to a rigid-sphere gas in which the external pressure is replaced by the thermal pressure.

It is more convenient to redefine the factor Y as $y = (b_0/V)\, Y$. Therefore

$$y = (1/\rho\kappa T)[T(\partial P/\partial T)_V - 1]$$

Since $y/\rho \to b_0$ as $\rho \to 0$, then

$$b_0 = B(T) + T(dB/dT) \tag{9}$$

where $B(T)$ is the second virial coefficient. It is worth noticing that b_0 is equal to the second virial coefficient when the system is composed of rigid spherical molecules, while with the inclusion of thermal pressure, an additional term $T(dB/dT)$ is added as a Taylor expansion term.

From Eq. (9) an expression for the molecular diameter as a function of temperature is directly obtained as

$$\sigma(T) = \{(3/2\pi N)[B(T) + T(dB/dT)]\}^{1/3} \tag{10}$$

From the equation of state (6), one immediately gets an expression for the second virial coefficient:

$$B^*(T^*) = (3/2\pi)(B_1/T^{*1/4} - C_1/T^{*3/4} + D_1/T^{*5/4}) \tag{11}$$

Then, from the above two equations we have

$$\sigma(T^*)/\sigma = [(3/8\pi)(3B_1/T^{*1/4} - C_1/T^{*3/4} - D_1/T^{*5/4})]^{1/3} \qquad (12)$$

Equation (12) gives the sphere diameter in reduced units as a function of the reduced temperature. In Eq. (12), σ is considered as the reference diameter obtained from viscosity data in the temperature range 300–1000 K.[18]

The Hugoniot calculations are strightforward because both the initial and final states are equilibrium states. From the equation of state (6) and Eq. (8) an expression for the excess internal energy (after subtracting the dilute gas contribution) in terms of density and temperature can be obtained. The dilute gas contribution to the internal energy is given by

$$E_{\text{dil}} = \frac{3}{2}RT + \frac{n}{2}RT + R\sum_{i=1}^{\alpha}\left(\frac{\Theta_{vi}}{2} + \frac{\Theta_{vi}}{\exp(\Theta_{vi}/T)-1}\right)$$

where n is the number of rotational degrees of freedom (two for linear molecules and three for nonlinear molecules). The third term in the above expression represents the vibrational energy, where Θ_v is the characteristic vibrational temperature ($\Theta_v = hv/k$) and α is the number of vibrational degrees of freedom. Values for Θ_v are listed in Table I.[19] Changes in the vibrational frequencies on compression are neglected.

Having both P and E in terms of ρ and T, one obtains the Hugoniot relation in terms of ρ and T. By choosing any value of ρ greater than ρ_0, one can solve for T by searching for the zero of the function

$$F(T) = \tfrac{1}{2}(P + P_0)(1/\rho_0 - 1/\rho) - (E - E_0)$$

Table I. "Reference" Potential Parameters and Characteristic Vibrational Temperature

	σ (Å)[a]	ε/k (K)[a]	Θ_v (K)
N_2	3.749	79.8	3374[b]
O_2	3.541	88.0	2273[c]
H_2	2.915	38.0	6340[d]
D_2	2.948	39.3	4395[d]
CH_4	3.796	144.0	4170; 2180(2); 4320(3); 1870(3)[c]
CO	3.706	88.0	3122[c]
CO_2	3.897	213.0	1890; 3360; 954(2)[c]

[a] Reference 18.
[b] Reference 19.
[c] Reference 9.
[d] Reference 12.

The input value for $\sigma(T)$ is varied along the Hugoniot until it matches the value predicted from Eq. (12). Values for σ evaluated from viscosity[18] are taken as the reference values. These values for different species are listed in Table I.

3. RESULTS AND DISCUSSION

Equations (11) and (12) are used to calculate the reduced second virial coefficient $B^*(T^*)$ and the reduced sphere diameter $\sigma(T^*)/\sigma$ as a function of the reduced temperature. Figures 1 and 2 along with Table II show these calculations compared with values of $B^*(T^*)$ given in Table IB of Hirschfelder *et al.*[18] and with values of $\sigma(T^*)/\sigma$ calculated from the same table. The two calculations are almost indistinguishable over a wide range of the reduced temperature. The second virial coefficient shown in Fig. 1 is negative at low temperatures and starts to change its sign at $T^* = 3.875$. It increases from large, negative values to positive, but with decreasing slope. It passes through a maximum at $T^* = 28.51$ and then decreases slightly with increasing T^*. The behavior of the second virial coefficient reflects the nature of the intermolecular potential. At low temperature, the contribution from the attractive part of the potential is important, while as the temperature increases, the repulsive part tends to be dominant.

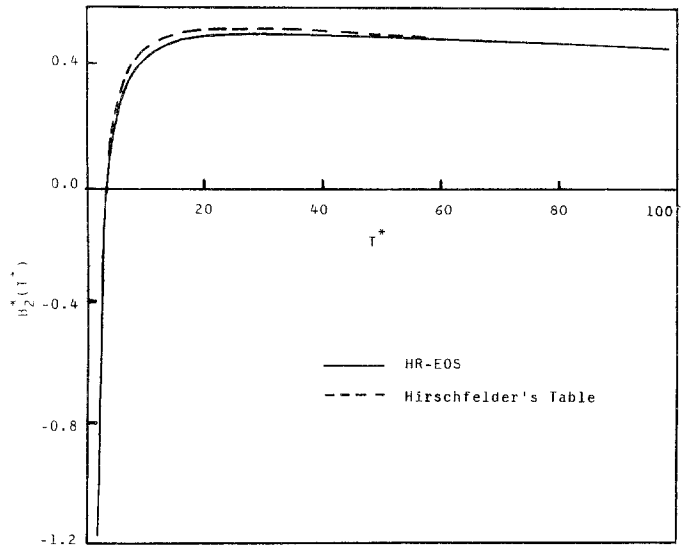

Fig. 1. Second virial coefficient in reduced units versus reduced temperature as calculated by (—) HR-EOS compared with that from (- -) HCB.

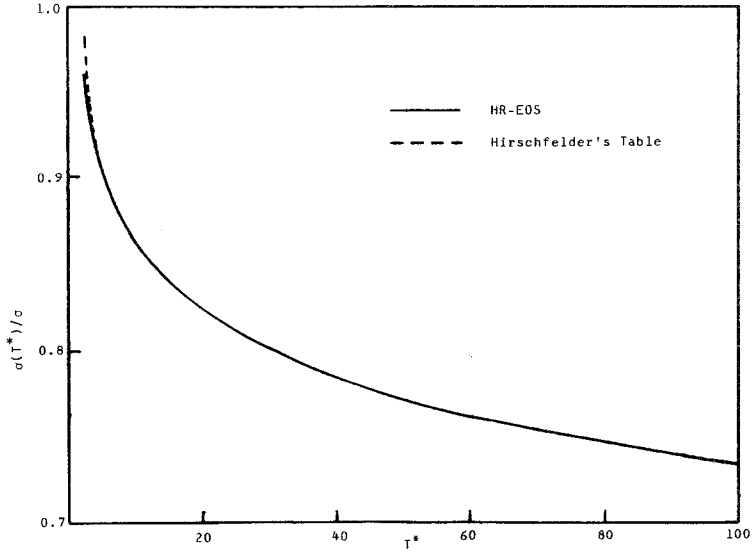

Fig. 2. Sphere diameter in reduced units versus reduced temperature as calculated by (—) HR-EOS compared with that from (- -) HCB.

Table II. The Second Virial Coefficient and Sphere Diameter in Reduced Units versus Reduced Temperature as Calculated by Hansen–Ree (HR) Equation of State and Those from Hirschfelder *et al.* (HCB)

T^*	$B_2^*(T^*)$		$\sigma(T^*)/\sigma$	
	HR	HCB	HR	HCB
2	−0.7683	−0.6276	0.9608	1.0021
4	0.0241	0.1154	0.9150	0.9190
6	0.2608	0.3229	0.8911	0.8908
8	0.3674	0.4134	0.8746	0.8732
10	0.4247	0.4609	0.8619	0.8603
20	0.5089	0.5253	0.8226	0.8213
30	0.5166	0.5269	0.7996	0.7986
40	0.5112	0.5186	0.7833	0.7826
50	0.5027	0.5084	0.7707	0.7705
60	0.4937	0.4982	0.7604	0.7599
70	0.4849	0.4887	0.7518	0.7501
80	0.4766	0.4798	0.7443	0.7439
90	0.4688	0.4716	0.7377	0.7374
100	0.4616	0.4641	0.7319	0.7316

In Fig. 2 the reduced molecular diameter shows a fast decrease with T^* until about $T^* \sim 20$. Then it starts to be a slowly decreasing function of temperature. This monotonic decrease of $\sigma(T^*)/\sigma$ as the temperature increases reflects the fact that at high temperature, molecules approach and scatter at much smaller distances.

Based upon a virial expansion in density and taking the reference state as a hard-sphere gas represented by the Percus–Yevick equation of state, Haar and Shenker[20] developed an expression for the sphere diameter as a function of temperature. Their calculations for $\sigma(T^*)/\sigma$ as function of T^* indicate that the sphere diameter is also a monotone decreasing function of the temperature.

The close agreement between our calculations and those from Hirschfelder *et al.* and the results of Haar and Shenker lead to confidence in our simple approach.

3.1. Nitrogen

The Hugoniot data for both N_2 and O_2 are presented as U_s versus U_p and P versus V/V_0 plots. In Fig. 3 the calculated U_s versus U_p Hugoniot

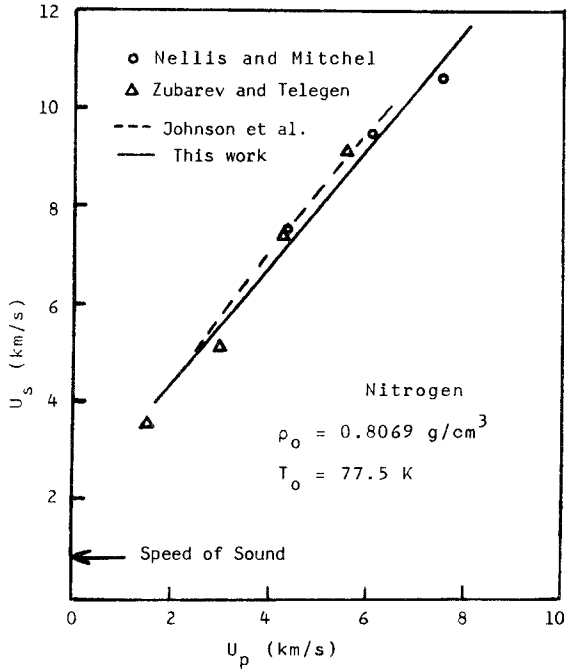

Fig. 3. Liquid N_2 Hugoniot; shock velocity versus mass velocity.

for N_2 is plotted along with the experimental data of Nellis and Mitchell[3] and Zubarev and Telegin,[2] where the initial state was $(\rho_0, T_0) = (0.808\ \text{g/cm}^3,\ 77.4\ \text{K})$. The same figure shows the theoretical calculations of Johnson *et al.*,[21] who used a scaled atom–atom (exp-6) potential with molecular dynamics. They produced an extensive set of molecular dynamics runs establishing the equation of state for dense N_2. They also demonstrated the existence of an effective spherical potential that models very accurately the equation of state of the anisotropic N_2 potential. The comparison with the experimental data and with Johnson's work shows a reasonable overall agreement.

Since a linear U_s versus U_p relationship is observed, the data were fitted by a linear least square fit to the relation

$$U_s = C + SU_p \tag{13}$$

Our data fit $U_s = 1.91 + 1.20U_p$ in the range $2.19 < U_p < 8.31$ km/sec and the two sets of experimental data[2,3] fit to $U_s = 2.09 + 1.17U_p$ in the range $1.17 < U_p < 7.54$ km/sec.

Since an infinitely weak shock is considered as a sound wave, then as $U_p \to 0$, C in Eq. (13) should be equal to the speed of sound. However, the intercept with the U_s axis defined by Eq. (13) predicts a higher value (see Fig. 3).

In Fig. 4 the P versus V/V_0 relation calculated with the present approach (using the Hansen–Ree equation of state and Enskog theory) is plotted along with the experimental results of Nellis and Mitchell[3] and Zubarev and Telegin.[2] The figure also shows the Hugoniot curve calculated by Ross and Ree[9] and that calculated by the Hansen–Ree equation of state with constant Lennard-Jones parameters ($\sigma = 3.64$ Å and $\varepsilon/k = 101.9$ K[22]).

As Fig. 4 indicates, the Hugoniot calculations based upon the Hansen–Ree equation of state with constant LJ parameters (curve 1 in Fig. 4) deviate drastically from the experimental data, predicting much higher pressure at high densities. This reflects the stiffness and inflexibility of the Lennard-Jones potential. However, when the shock compression calculations are refined by allowing σ to be a function of the temperature along the Hugoniot using Enskog theory, the disagreement is noticeably reduced (curve 3 in Fig. 4). Our calculations are in a good agreement with the experimental data of Zubarev and Telegin up to about 150 kbar. In the range $V/V_0 = 0.425$ to 0.375 our calculations predict slightly lower pressure. Then the calculations return to a good agreement with the experimental work of Nellis and Mitchell up to about 650 kbar.

Shock compression calculations of Ross and Ree based upon a corresponding state law in conjunction with the exp-6 intermolecular

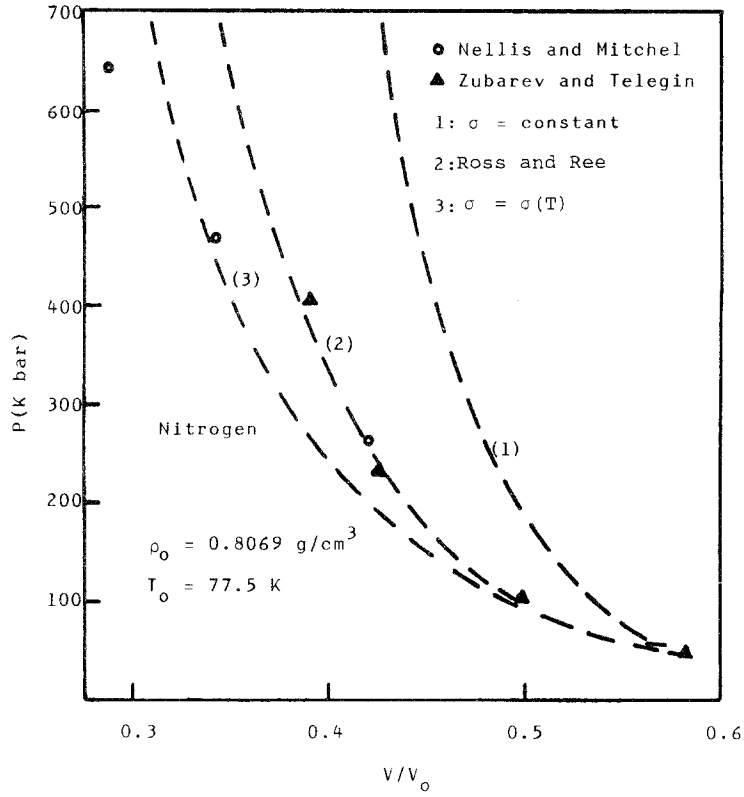

Fig. 4. Liquid N_2 Hugoniot; pressure versus compression.

potential appear to agree well with the experimental data up to a pressure of 400 kbar. Above this pressure their calculations deviate sharply, predicting higher pressure (curve 2 in Fig. 4). They suggested that this divergence is probably due to the dissociation of N_2 molecules. Our calculations gave an estimated total internal energy to be 3.43×10^{-17} J per molecule at $P \sim 440$ kbar, while the dissociation energy of N_2 is about 1.6×10^{-18} J per molecule.[23] This supports the conclusion of Ross and Ree.

Comparison between esperimental T versus P data of Voskoboinikov *et al.*[24] and different theoretical calculations is made in Fig. 5. As the figure indicates, both theory and experiment reveal an approximately linear T versus P relationship. However, our calculations and those of Ross and Ree deviate at higher pressures, predicting higher temperatures, while those of Johnson *et al.*[21] are in good agreement with experiment. Their

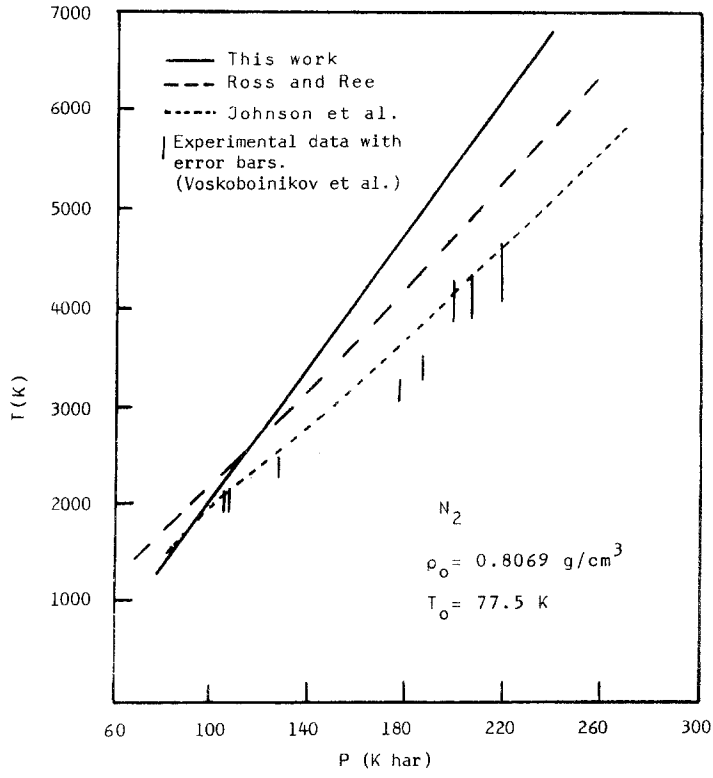

Fig. 5. Shock temperature versus shock pressure for liquid N_2.

calculations are based upon the Mansoori–Canfield–Ross fluid perturbation theory[25] assuming an effective spherical (exp-6) potential for N_2. The best effective spherical potential for N_2 was obtained by taking the median average over angles. The present model and that of Ross and Ree are adequate for spherically symmetric systems.

3.2. Oxygen

The shock Hugoniot for oxygen in the U_s versus U_p plane is depicted in Fig. 6, where the present calculations are compared with the experimental work of Nellis and Mitchell and of Wackerle *et al.*[3] Our results fit $U_s = 2.143 + 1.184U_p$ in the range $1.66 < U_p < 7.24$ km/sec, while the experimental data give $U_s = 2.327 + 1.215U_p$ for $2.6 < U_p < 6.8$ km/sec.

In Fig. 7 the calculated shock Hugoniot along with the experimental data[3] are plotted in the P versus V/V_0 plane. As the figure indicates, the

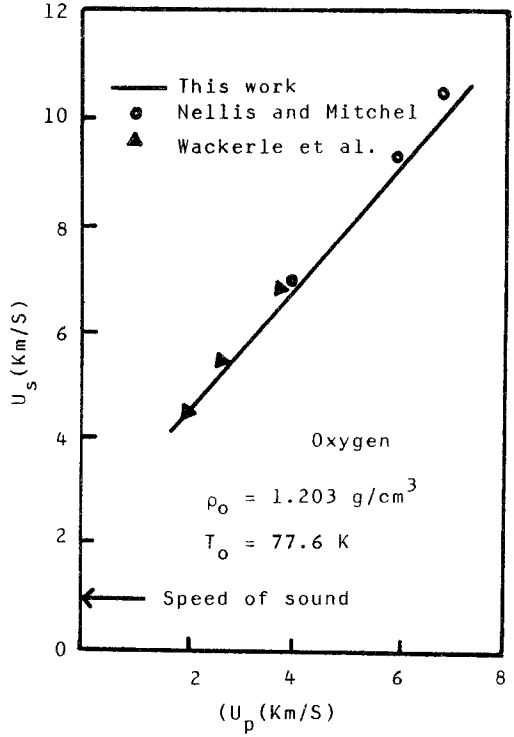

Fig. 6. Liquid O_2 Hugoniot; shock velocity versus mass velocity.

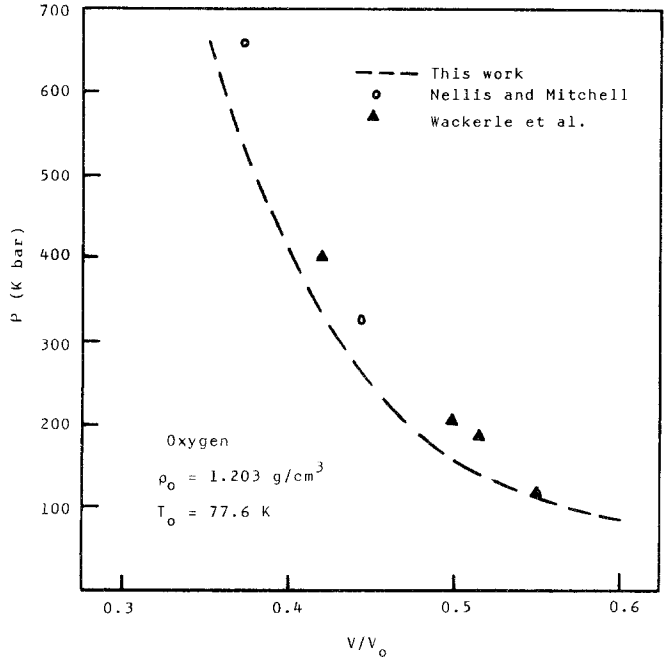

Fig. 7. Liquid O_2 Hugoniot; pressure versus compression.

theoretical Hugoniot curve is located slightly lower than the experimental Hugoniot curve. This suggests that a slight adjustment of the reference Lennard-Jones parameters for O_2 ($\sigma = 3.541$ Å and $\varepsilon/k = 88$ K[18]) would bring the calculated and the experimental curves into better agreement.

The temperature versus pressure relation for O_2 as calculated by the present model along with those calculated by Ross and Ree[9] are shown in Fig. 8. The two calculations reveal an approximately linear relationship. However, as the pressure increases, our model predicts higher temperature.

3.3. Hydrogen and Deuterium

Ross *et al.*[12] used recent shock data to determine an improved effective intermolecular potential and an equation of state for molecular hydrogen valid over a broad range of conditions. They analyzed the shock compression data using several different potentials. Through these analyses, they found a simple three-parameter potential that can explain the experimental data for H_2 quite well. This potential has the form of the exp-6 with the parameters $\varepsilon/k = 36.41$, $r^* = 3.43$ Å, and $\alpha = 11.1$.

The thermodynamic properties were calculated using the Helmholtz free energy based upon the fluid variational theory. The expression for the

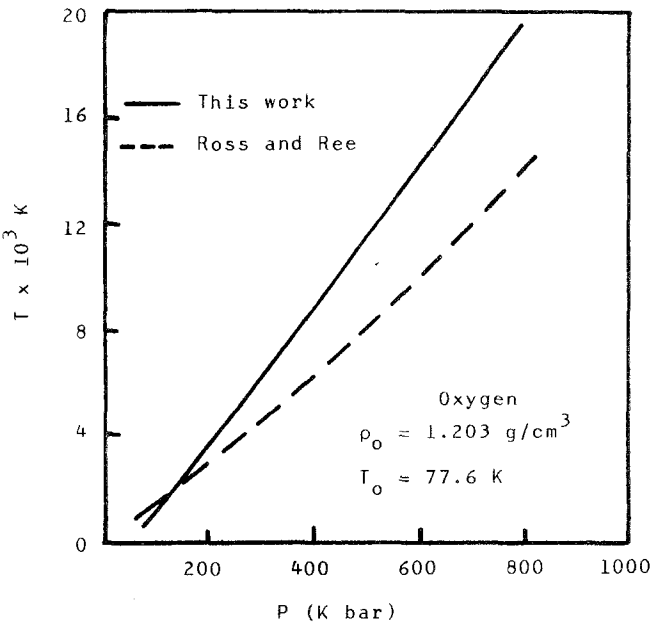

Fig. 8. Shock temperature versus shock pressure for liquid O_2.

Helmholtz free energy contains an expression for the hard-sphere excess free energy. The hard-sphere diameter was treated as the only variational parameter, which was determined by minimizing the Helmholtz free energy.

Using the initial state $(V_0, T_0) = (28.422\ \text{cm}^3/\text{mole},\ 20.35\ \text{K})$ for H_2 and $(V_0, T_0) = (23.64\ \text{cm}^3/\text{mole},\ 20\ \text{K})$ for D_2, their shock Hugoniot calculations for H_2 and D_2 agree satisfactorily with the experimental data over the entire experimental range.

Applying the same procedure used for N_2 and O_2 (namely, adjusting the parameter σ along the Hugoniot so that its value matches that predicted by the Enskog theory) to H_2 and D_2 produced poor results (about 25–45% difference in pressure over the experimental range[3]). These difficulties are attributable to the fact that H_2 molecular interactions in the condensed phase contain an essential many-body contribution. The persent model is based upon the second virial coefficient and consequently concerns mainly two-body molecular interactions. Therefore, instead of calculating the shock Hugoniot for H_2 and D_2, we compare three different theoretical calculations (Figs. 9 and 10) for the reduced "sphere diameter" versus reduced temperature: (i) those values of $\sigma(T^*)/\sigma$ that are required to match the experimental data, (ii) those calculated using the Enskog theory, and (iii) values of hard-sphere diameter calculated by Ross *et al.* along the Hugoniot through the minimization of the Helmholtz free energy. To transfer temperature and "sphere diameter" into reduced values, the pair potential parameters used are $(\sigma, \varepsilon/k) = (2.915\ \text{Å},\ 38\ \text{K})$ for H_2 and

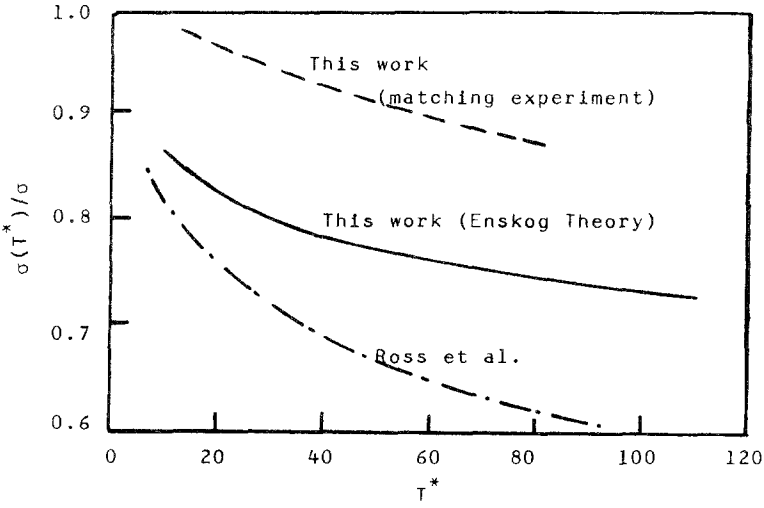

Fig. 9. Reduced sphere diameter versus reduced temperature for liquid H_2.

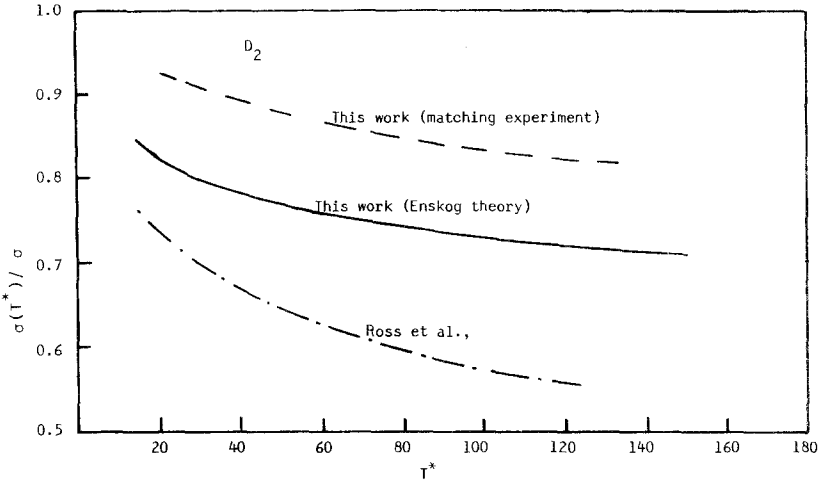

Fig. 10. Reduced sphere diameter versus reduced temperature for liquid D_2.

$(\sigma, \varepsilon/k) = (2.948\ \text{Å},\ 39.3\ \text{K})$ for D_2.[18] The ideal gas contribution to the internal energy was taken to be $3.5RT$ for both H_2 and D_2.

As both figures indicate, the three calculations show a monotone decrease of $\sigma(T^*)/\sigma$ as T^* increases. However, the curve corresponding to matching the experimental data is almost parallel to that computed by the Enskog theory, while that computed by Ross *et al.*[12] decreases a little faster than the other two.

3.4. Methane

The calculated U_s versus U_p shock Hugoniot of liquid CH_4 along with the experimental data of Nellis *et al.*[4] are illustrated in Fig. 11. The initial state for these calculations is $(V_0, T_0) = (37.94\ \text{cm}^3/\text{mole},\ 111.3\ \text{K})$.

As the comparison indicates, the Hugoniot calculated using this simple approach is in a good agreement with the experimental data. The experimental data fit $U_s = 2.625 + 1.200U_p$ in the range $2.222 < U_p < 8.341$ km/sec, while the present calculations fit $U_s = 2.893 + 1.153U_p$ in the range $2.415 < U_p < 8.066$ km/sec.

In Fig. 12 the P versus V/V_0 Hugoniot for CH_4 calculated with the present approach is compared with that calculated by Ross and Ree using the corresponding state theory.[9] The experimental data are also shown. As the figure indicates, our calculations agree closely with the experimental data. However, the Hugoniot calculated by Ross and Ree agrees with the experimental Hugoniot up to about 230 kbar and then starts to deviate, predicting much higher pressure. They suggested that the reason behind the

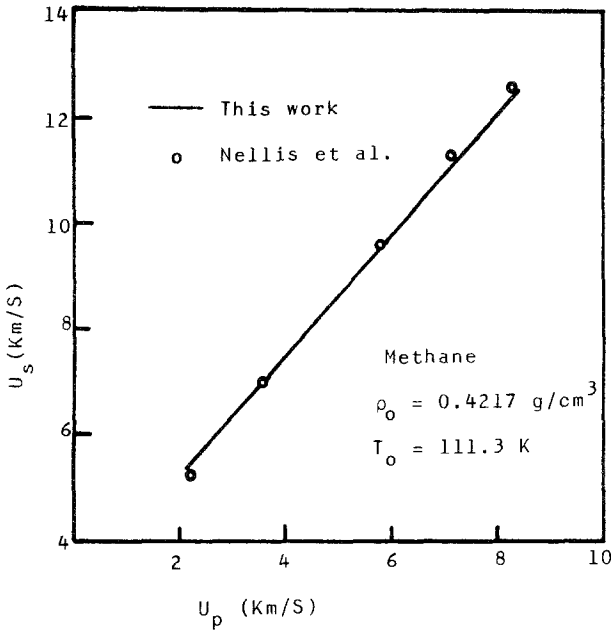

Fig. 11. Liquid CH_4 Hugoniot; shock velocity versus mass velocity.

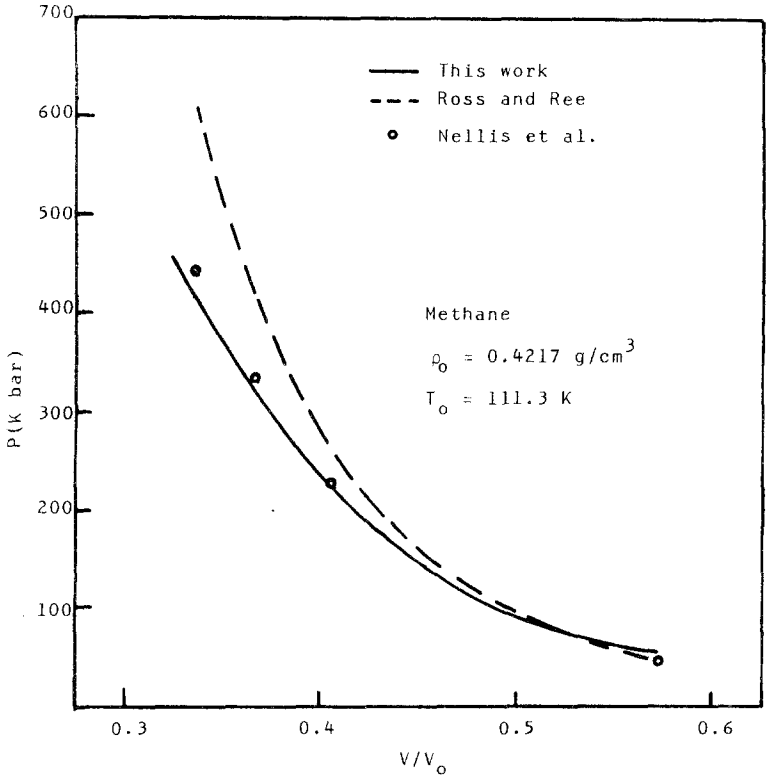

Fig. 12. Liquid CH_4 Hugoniot; pressure versus compression.

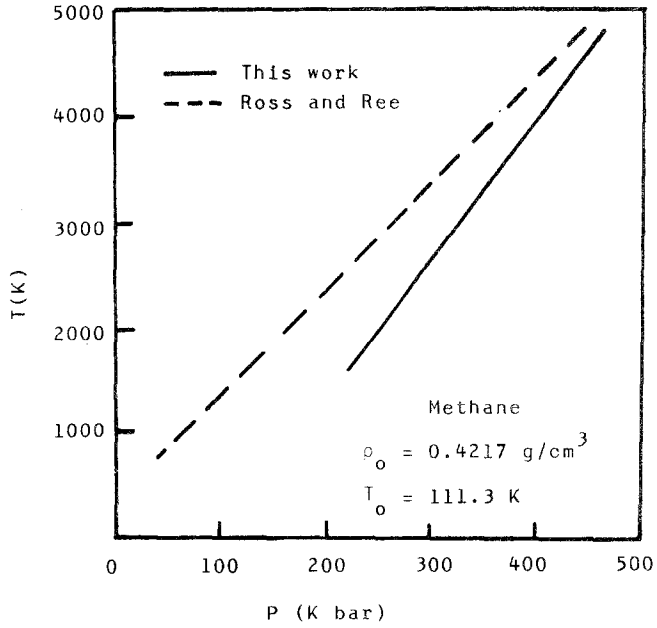

Fig. 13. Shock temperature versus pressure for liquid CH_4.

deviation is the tendency of CH_4 to dissociate into elemental carbon and molecular hydrogen at these conditions.

Our calculations for the temperature versus pressure relation are compared with those calculated by Ross and Ree in Fig. 13. Both calculations reveal an approximately linear relationship.

3.5. Carbon Monoxide

The *P–V* Hugoniot for CO calculated with the present approach (curve 4 in Fig. 14) is superimposed on top of the calculations of Nellis *et al.*[4] in Fig. 14. Their experimental data are also shown.

It has been suggested[4] that CO at high temperature and pressure decomposes into gaseous species and elemental carbon. Therefore, Nellis *et al.* proposed three different theoretical Hugoniots: Hugoniot 1 in Fig. 14 represents the nonreactive case calculated by the corresponding state theory; Hugoniot 2 allows chemical reactions, but without the formation of the diamond phase; and Hugoniot 3 assumes complete chemical equilibrium where the formation of both graphite and diamond phases are permitted. Their analysis utilizes three gaseous products (CO, CO_2, and O_2) and two solid phases (graphite and diamond).

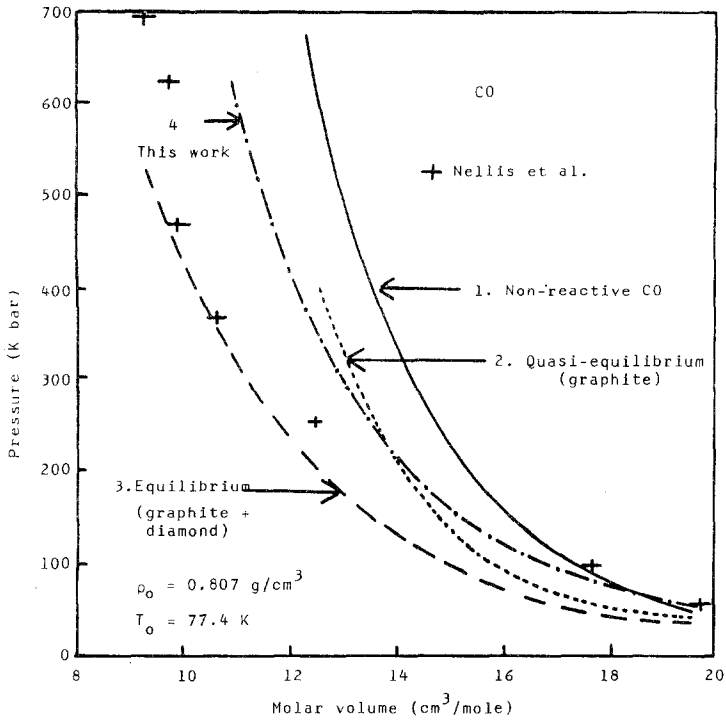

Fig. 14. Liquid CO Hugoniot; shock pressure versus molar volume as calculated by four theoretical models

At low pressure (up to about 100 kbar) the experimental data are close to the nonreactive Hugoniots (curves 1 and 4 in Fig. 14). Our calculations assume that molecules do not dissociate. As the pressure increases, our calculations become closer to the experimental results than do Hugoniots 1 and 2 of Nellis *et al.* In the pressure range 250–500 kbar the experimental data are closer to Hugoniot 3, while at higher pressure (600–700 kbar) they lie between Hugoniots 3 and 4.

The present calculations predict the early dissociation of CO. The pronounced deviation between the calculations (nonreactive Hugoniots 1 and 4 in Fig. 14) and experimental data is probably due to the existence of many different species (three gaseous products and two solid phases); the anisotropy permits closer packing of molecules.

The temperature versus pressure relation calculated with the present approach is also superimposed on top of the calculations of Nellis *et al.*[4] in Fig. 15. As the figure indicates, curve 3, which assumes the existence of

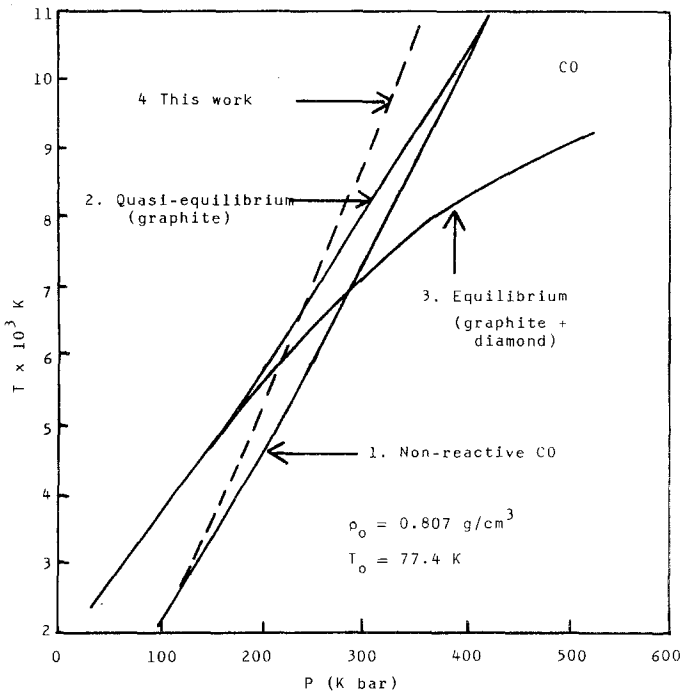

Fig. 15. Shock temperature versus shock pressure for liquid CO as calculated by four theoretical models.

graphite and diamond, exhibits curvature at the high-pressure end. The other calculations (including ours) reveal an approximately linear relationship.

3.6. Carbon Dioxide

For carbond dioxide, the experimental work of Zubarev and Telegin[2] is the only available experimental data. The initial state they used is

Table III. Experimental CO_2 Hugoniot of Zubarev and Telegin with the Correct Pressure and Density

U_p (km/sec)	U_s (km/sec)	ρ(g/cm^3)	P (kbar)
1.03	3.57	2.19	57.2
2.14	5.38	2.59	179.6
3.68	7.71	2.98	441.9
4.79	9.05	3.31	675.5

$(\rho_0, T_0) = (1.56\ \text{g/cm}^3, 196\ \text{K})$. This state corresponds to solid phase near the sublimation point at 1 atm.

As Ross and Ree[9] noticed, the Hugoniot pressure and density calculated by Zubarev and Telegin using their experimental data for shock and particle velocity are incorrect. They used an initial density of about $1.45\ \text{g/cm}^3$, while the correct value is $1.56\ \text{g/cm}^3$. Therefore, to compare the present calculations with the correct experimental data we recalculated pressure and density using the experimental data for U_s and U_p with the initial state $(V_0, T_0) = (1.56\ \text{g/cm}^3, 196\ \text{K})$. These data are depicted in Table III.

By varying σ so that it matches the value predicted by the Enskog theory, we found that for CO_2, in particular, σ is almost constant along the Hugoniot. The Lennard-Jones parameters that produce good agreement with the experimental results are $(\varepsilon/k, \sigma) = (213\ \text{K}, 3.53\ \text{Å})$. This value for σ is about 9% less than its value obtained from viscosity.[18]

The Hugoniot calculated with these parameters is presented as U_s versus U_p and P versus V/V_0 plots in Figs. 16 and 17, respectively. The experimental data of Zubarev and Telegin are also shown. As the figures indicate, the calculations are in good agreement with the experiment. The U_s versus U_p calculations fit $U_s = 1.85 + 1.54U_s$ in the range

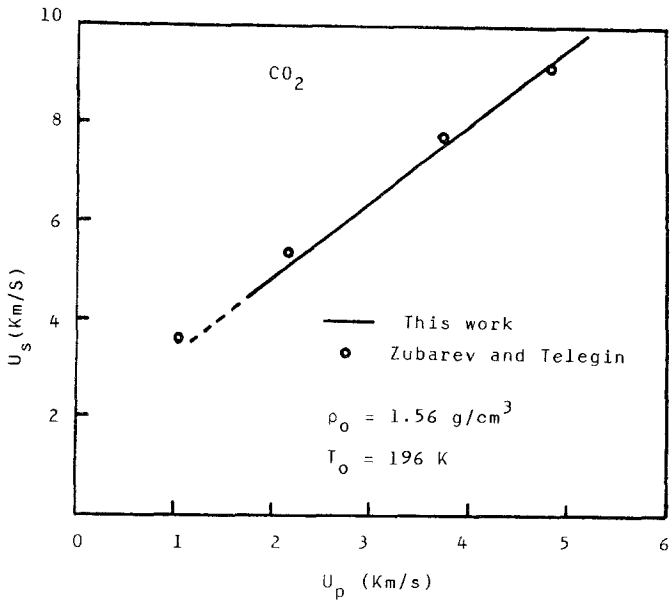

Fig. 16. Solid CO_2 Hugoniot; shock velocity versus mass velocity.

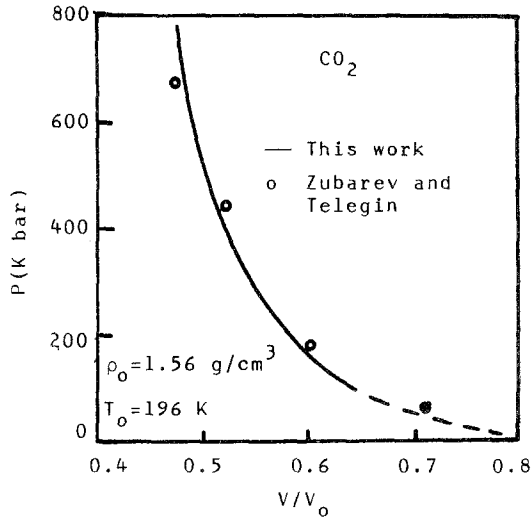

Fig. 17. Solid CO_2 Hugoniot; pressure versus compression.

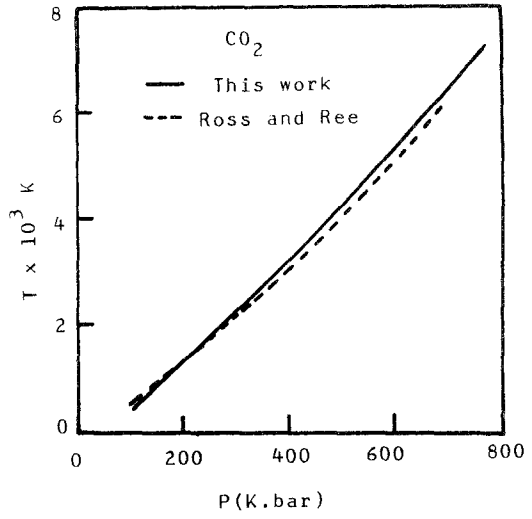

Fig. 18. Shock temperature versus pressure for solid CO_2.

$1.63 < U_p < 5.15$ km/sec, while the experimental data fit $U_s = 2.16 + 1.47U_s$ in the range $1.03 < U_p < 4.79$ km/sec.

In Fig. 18, the temperature versus pressure relation calculated with the present approach is compared with that calculated by Ross and Ree using the corresponding state theory.[9] The two calculations are almost identical. They both reveal an approximately linear relationship.

4. CONCLUSION

The fact that at high temperature, molecules approach and scatter at much smaller distances led to the idea of applying the Enskog theory to calculate the molecular diameter as a function of temperature along the Hugoniot. In conjunction with an accurate analytic represention of the Lennard-Jones fluid, we have presented a simple, yet reliable recipe to calculate shock compression of simple molecules. Results are in reasonable agreement with experimental data and comparable to those from more complicated calculations. However, the limitation of this approach is the requirement of accurate values for the "reference" potential parameters. The model is adequate to describe spherically symmetric systems and works better when the molecular interactions are mainly two-body interactions.

REFERENCES

1. C. L. Mader, *Numerical Modeling of Detonations* (University of California Press, Berkeley, 1979).
2. V. N. Zubarev and G. S. Telegin, *Sov. Phys. Dokl.* **7**:34 (1962).
3. W. J. Nellis and A. C. Mitchell, *J. Chem. Phys.* **73**:6137 (1980).
4. W. J. Nellis, F. H. Ree, M. Van Thiel, and C. Mitchell, *J. Chem. Phys.* **75**:3055 (1981).
5. W. J. Nellis, J. C. Mitchell, M. Van Thiel, G. J. Devine, and R. J. Trainor, *J. Chem. Phys.* **79**:1480 (1983).
6. M. Ross, *J. Chem. Phys.* **60**:3634 (1974).
7. M. Ross, *J. Chem. Phys.* **73**:4445 (1980).
8. G. I. Kerley and J. Abdallah, Jr., *J. Chem. Phys.* **73**:5337 (1980).
9. M. Ross and F. H. Ree, *J. Chem. Phys.* **73**:6146 (1980).
10. D. A. Young and M. Ross, *J. Chem. Phys.* **74**:6950 (1981).
11. W. J. Nellis, M. Ross, A. C. Mitchell, and M. Van Thiel, *Phys. Rev. A* **27**:608 (1983).
12. M. Ross, F. H. Ree, and D. A. Young, *J. Chem. Phys.* **73**:1487 (1983).
13. D. Henderson and P. J. Leonard, in *Physical Chemistry—An Advanced Treatise*, Vol. 8 (1971), 413.
14. J. Hansen, *Phys. Rev. A* **2**:221 (1970).
15. F. H. Ree, *J. Chem. Phys.* **73**:5401 (1980).
16. M. S. Abdelazim and W. G. Hoover, *J. Phys. Chem.* **87**:2795 (1983).
17. M. S. Abdelazim, in *Proceeding of the 10th International Colloquium on Dynamics of Explosives and Reactives Systems, Berkeley, August 4–9, 1985*, in press.

18. J. O. Hirschfelder, C. F. Curtiss, and R. B. Bird, *Molecular Theory of Gases and Liquids* (Wiley, New York, 1964).
19. D. A. McQuarrie, *Statistical Mechanics* (Harper & Row, New York, 1976).
20. L. Haar and S. H. Shenker, *J. Chem. Phys.* **55**:4951 (1971).
21. J. D. Johnson, M. S. Show, and B. L. Holian, *J. Chem. Phys.* **80**:1279 (1984).
22. F. H. Ree, *J. Chem. Phys.* **81**:1251 (1984).
23. A. G. Gaydon, *Dissociation Energies and Spectra of Diatomic Molecules* (Chapman and Hall, 1953).
24. I. M. Voskonoinikov, M. F. Gogula, and Yu. A. Dolgoborodov, *Sov. Phys. Dokl.* **24**:375 (1979).
25. M. Ross, *J. Chem. Phys.* **71**:1567 (1979).